Langmuir
Article
pubs.acs.org/Langmuir

Chelating Langmuir−Blodgett Film: A New Versatile Chemiluminescent Sensing Layer for Biosensor Applications

Aurélie A-M. Santafé, Loïc J. Blum, Christophe A. Marquette, and Agnès P. Girard-Egrot*

Institut de Chimie et Biochimie Moléculaires et Supramoléculaires (ICBMS), CNRS, CPE Lyon, INSA de Lyon, UMR 5246, Université Lyon 1, Villeurbanne, Université de Lyon, F-69622, Lyon, France

Received July 20, 2009. Revised Manuscript Received November 20, 2009

The present study reports the achievement of a new chemiluminescent sensing layer able to simultaneously (i) play an active role on ligand immobilization and (ii) serve as a catalyst in detection processes for label-free biosensor applications. This new type of active Langmuir−Blodgett (LB) monolayer has been designed by using a chelating lipid (Ni-NTA-DOGS). Thanks to the chelated metallic cation, this peculiar lipid exhibits luminol chemiluminescence catalysis properties in the presence of hydrogen peroxide. Upon biomolecule interaction through imidazole ring chelation (mediated by the metallic cation bound to the lipid headgroup), the chemiluminescent signal can be modulated. The first chemiluminescent signal acquisition experiments have shown a strong and homogeneous signal of the chelating layer. Upon histamine interactions, a histidine derivative used as a marker of fresh food quality, we succeeded in obtaining as a proof of concept a chemiluminescent signal variation without any derivatization of the target molecule. This signal variation was shown to be directly correlated to the histamine concentration with a limit of detection of 2 μg/mL.

Introduction

In the wide domain of analysis, the willingness to develop some reliable and efficient systems based on fundamental characteristics such as sensitivity, specificity, miniaturization, rapidity, and multiplexing led to the development of biosensors and biochips. The performance of a biosensor is closely linked to the properties of the sensitive layer and the quality of its association with the transducer. Current achievements follow the marked trend toward miniaturization of recognition systems.[1] Molecular scale patterning of the sensitive layer is therefore a crucial step in sensor miniaturization.

The Langmuir−Blodgett (LB) technique[2−4] offers the possibility to prepare, by molecular self-assembling, ultrathin lipid layers[5−7] suitable for nanoscale applications requiring a controlled biomolecule immobilization.[8,9] After functionalization, LB films allow the building up of nanometer-thick organized sensing layers, which are powerful tools for molecular interaction investigations.[10,11] More particularly, the study of protein−ligand interactions can be envisaged after immobilization of biomolecules presenting specific recognition properties via covalent coupling[12−14] or specific ligand/receptor-mediated binding.[15−17] Nevertheless, one of the major issues in using surface sensitive techniques for investigating protein/protein interactions remains the optimal functional orientation of the immobilized bioreceptor, a problem that can be overcome by using functionalized lipids.[18]

Lipids presenting a chelating headgroup, namely, chelating lipids, have been extensively studied in the past 30 years. Their concept is based on immobilized metal ion affinity chromatography (IMAC), a purification technique using a chelated ion able to bind histidine residues present at the protein surface, chemically grafted or overexpressed in fusion proteins (His-tagged proteins).[19] Suitable to coat materials, these lipids have been used to immobilize proteins and functionalize different systems: liposomes for drug delivery (targeting system with inserted antibodies),[20,21] lipid surfaces for bioreceptor immobilization,[22] fluid functionalized interface for two-dimensional (2D) protein crystallization.[23−26] Nowadays, many kinds of lipids presenting a chelating headgroup

*To whom correspondence should be addressed. E-mail: agnes.egrot@univ-lyon1.fr. Phone: +33 (0)4.72.44.85.32. Fax: +33 (0)4.72.44.79.70.

(1) Angenendt, P. *Drug Discovery Today* **2005**, *10*, 503–511.
(2) Ulman, A. *An Introduction to Ultra Thin Organic Films from Langmuir−Blodgett to Self-Assembly*; Academic Press, Inc.: San Diego, CA, 1991.
(3) Gaines, G. L. *Insoluble Monolayers at Liquid−Gas Interface*; Interscience Publishers: New York, 1966.
(4) Roberts, G. *Langmuir−Blodgett Films*; Plenum Press: New York, 1990.
(5) Morélis, R.; Girard-Egrot, A. P.; Coulet, P. R. *Langmuir* **1993**, *9*, 3101–3106.
(6) Girard-Egrot, A. P.; Morélis, R. M.; Coulet, P. R. *Langmuir* **1996**, *12*, 778–783.
(7) Girard-Egrot, A. P.; Morélis, R. M.; Coulet, P. R. *Langmuir* **1993**, *9*, 3107–3110.
(8) Girard-Egrot, A. P.; Godoy, S.; Blum, L. J. *Adv. Colloid Interface Sci.* **2005**, *116*, 205–225.
(9) Girard-Egrot, A. P.; Blum, L. J. Langmuir−Blodgett technique for synthesis of biomimetic lipid membranes. In *Fundamental Biomedical Technologies*; Martin, D. K., Ed.; Springer Science+Business Media, LLC: New York, 2007; pp 23−74.
(10) Godoy, S.; Violot, S.; Boullanger, P.; Bouchu, M. N.; Leca-Bouvier, B. D.; Blum, L. J.; Girard-Egrot, A. P. *ChemBioChem* **2005**, *6*, 395–404.
(11) Godoy, S.; Chauvet, J.-P.; Boullanger, P.; Blum, L. J.; Girard-Egrot, A. P. *Langmuir* **2003**, *19*, 5448–5456.
(12) Zhang, A.; Hou, Y.; Jaffrezic-Renault, N.; Wan, J.; Soldatkin, A.; Chovelon, J.-M. *Biosens. Bioelectron.* **2002**, *56*, 157–158.
(13) Wan, K.; Chovelon, J. M.; Jaffrezic-Renault, N. *Talanta* **2000**, *52*, 663–670.
(14) Hou, Y.; Tlili, C.; Jaffrezic-Renault, N.; Zhang, A.; Martelet, C.; Ponsonnet, L.; Errachid, A.; samitier, J.; Bausells, J. *Biosens. Bioelectron.* **2004**, *20*, 1126–1133.
(15) Vikholm, I.; Viitala, T.; Albers, W. M.; Peltonen, J. *Biochim. Biophys. Acta, Biomembr.* **1999**, *1421*, 39–52.
(16) Vikholm, I.; Albers, W. M. *Langmuir* **1998**, *14*, 3865–3872.
(17) Ihalainen, P.; Peltonen, J. *Langmuir* **2002**, *18*, 4953–4962.
(18) Dorn, I.; Pawlitschko, K.; Pettinger, S.; Tampe, R. *Biol. Chem.* **1998**, *379*, 1151–1159.
(19) Schmitt, L.; Dietrich, C.; Tampe, R. *J. Am. Chem. Soc.* **1994**, *116*, 8485–8491.
(20) Chikh, G.; Li, W.; Schutze-Redelmeier, M.; Meunier, J.; Bally, M. *Biochim. Biophys. Acta, Biomembr.* **2002**, *1567*, 204–212.
(21) Nielsen, U.; Kirpotin, D.; Pickering, E.; Drummond, D.; Marks, J. D. *BMC Immunol.* **2006**, *7*, 24.
(22) Nye, J. A.; Groves, J. T. *Langmuir* **2008**, *24*, 4145–4149.
(23) Maloney, K.; Schief, W.; Pack, D.; Frey, W.; Arnold, F.; Vogel, V. *Coord. Chem. Rev.* **1999**, *183*, 3–18.
(24) Kubalek, E.; Legrice, S.; Brown, P. *J. Struct. Biol.* **1994**, *113*, 117–123.
(25) Pack, D.; Chen, G.; Maloney, K.; Chen, C.; Arnold, F. *J. Am. Chem. Soc.* **1997**, *119*, 2479–2487.
(26) Frey, W.; Schief, W.; Pack, D.; Chen, C.; Chilkoti, A.; Stayton, P.; Vogel, V.; Arnold, F. *Proc. Nat. Acad. Sci. U.S.A.* **1996**, *93*, 4937–4941.

can be found, generally built with either one or more iminodiacetate (IDA)[23,25] or nitrilotriacetic (NTA)[27,28] moieties associating a metallic cation (Ni^{2+}, Cu^{2+} or Zn^{2+}), a spacer, and two lipid tails with different unsaturation and carbon lengths on a glycerol backbone. The main interest of using these lipids in the surface functionalization lies on the versatility and the reversibility of the immobilization, and the protein orientation capability.[19] The orientation of an immobilized protein, an enzyme for instance, can affect the substrate access to its active site, hence its activity. By providing a well-defined orientation, chelating lipid headgroup/His-tag interactions provide an optimal functionality of the immobilized protein.[28]

The binding of a His-tagged molecule to a chelating solid surface has been characterized using numerous techniques, including surface plasmon resonance (SPR),[29,30] total internal reflection fluorescence,[31] resonant mirror,[27] bioluminescence,[30] X-ray photoelectron and correlation spectroscopies,[32] and atomic force microscopy (AFM).[33]

In this work, we propose a new label-free detection method based on molecule/metal chelate interactions using a chelating lipid LB film as the nanometer-thick immobilization matrix and the luminol chemiluminescence (CL) reaction as the detection system. Indeed, this reaction can be catalyzed either by enzymes (horseradish peroxidase (HRP), microperoxidases,[34] etc.) or by transition metal cations free or complexed to an organic or inorganic ligand. In this work, the bivalent metallic cation retained on the LB film chelating lipid headgroup plays a double role: (i) it allows molecule immobilization on the film surface (His-tagged or naturally histidine-enriched proteins, histidine, and phosphate or cystine/cysteine derivates), and (ii) it catalyzes the luminol CL reaction. The main advantage of the CL reaction of luminol for the design of biochips is its high sensitivity. For this reason, many sensors based on the luminol chemiluminescent and electrochemiluminescent reactions have been designed, and analytical applications relying on enzyme biosensors, immunochemical biosensors, DNA biosensors, and biochips have been recently reviewed.[34,35] Our approach combines the advantages of an organized sensing layer at the nanoscale level and the high sensitivity detection of the CL reaction. Providing a well-defined orientation of all chelated proteins to ensure their optimal functional properties, this new type of sensor offers a good comprise between sensitivity, variety of chelated materials, and performance. Upon interactions, the cation involved in the multiple chelation between the lipid and the immobilized molecules will no longer be available to catalyze the luminol CL reaction, leading to a decrease of the emitted light signal. In the case of bioreceptor immobilization, a new variation of the CL signal will be expected after ligand/receptor recognition due to a direct modification of the cation microenvironment.

In order to demonstrate the possibility to achieve a CL-supported monolayer and to record a CL signal variation upon molecule interaction, histamine has been used as model. Histamine is a degradation product of histidine. It is currently used as an indicator of deterioration in food, and frequently regarded as one of the biomarkers for quality control during food production and transportation. The procedure for histamine determination and that of other biogenic amines is usually chromatographic techniques using spectrometry or fluorescence derivatization, making it a time-consuming and expensive analysis.[36] While high-performance liquid chromatography (HPLC) is reliable, although sometimes bringing too much unnecessary information, this tool lacks rapidity and convenience. For these reasons, fast histamine determination with various biosensors (enzyme-based amperometric biosensors[37−39] or whole-cell-based biosensors)[40,41] is preferred because of their inherent fast responses in addition to the absence of sample pretreatment. However, enzyme-based amperometric biosensors reveal serious disadvantages with respect to substrate specificity.[42,43] On the positive side, such biosensors are adapted for flow injection analysis (FIA)[44,45] with the known advantage of continuous monitoring of many samples in a reproducible and user-friendly manner. Recently, chemical sensors for histamine detection based on ion-selective electrodes,[46,47] interactions with metallic porphyrins containing Cu^{2+} and Zn^{2+},[48] or using specific recognition films of molecularly imprinted polymers (MIPs) have been developed.[49] To our knowledge, only one CL sensor using immobilized histamine oxidase and peroxidase with a high detection limit has been documented.[50] In the present work, the preservation of the imidazole ring originated from histidine authorizes chelation with the lipid headgroup mediated by a metallic cation such as the nickel ion. A CL variation is therefore expected upon histamine interaction and is hopefully quantitatively related to the amount retained at the surface of the supported monolayer. Regardless of the demonstration of the feasibility to use CL supported monolayers as a label-free detection method to investigate molecular interactions, this approach can be promising to detect histamine without a preliminary derivatization procedure.

Materials and Methods

Materials. Silica substrates n-type 1.1.1 were directly purchased from Good Fellow (U.K.). They are made of one copper side and one silica side. Chloroform and dichloromethane, both for analysis (99.5%), were purchased from Carlo Erba (France). Sodium hydrogenocarbonate for analysis was provided from Chimie Plus (France). Copper chloride, zinc chloride for analysis,

(27) Altin, J.; White, F.; Easton, C. *Biochim. Biophys. Acta, Biomembr.* **2001**, *1513*, 131–148.
(28) Kent, M.; Yim, H.; Sasaki, D.; Satija, S.; Majewski, J.; Gog, T. *Langmuir* **2004**, *20*, 2819–2829.
(29) Stora, T.; Dienes, Z.; Vogel, H.; Duschl, C. *Langmuir* **2000**, *16*, 5471–5478.
(30) Ho, C.; Limberis, L.; Caldwell, K.; Stewart, R. *Langmuir* **1998**, *14*, 3889–3894.
(31) Schmid, E.; Keller, T.; Dienes, Z.; Vogel, H. *Anal. Chem.* **1997**, *69*, 1979–1985.
(32) Davis, J.; Glidle, A.; Cass, A.; Zhang, J.; Cooper, J. *J. Am. Chem. Soc.* **1999**, *121*, 4302–4303.
(33) Gizeli, E.; Glad, J. *Anal. Chem.* **2004**, *76*, 3995–4001.
(34) Marquette, C. A.; Blum, L. J. *Anal. Bioanal. Chem.* **2006**, *385*, 546–554.
(35) Marquette, C. A.; Blum, L. J. *Anal. Bioanal. Chem.* **2008**, *390*, 155–168.
(36) Peng, J.; Fang, K.; Me, D.; Ding, B.; Yin, J.; Cui, X.; Zhang, Y.; Liu, J. *J. Chromatogr. A* **2008**, *1209*, 70–75.
(37) Yamada, R.; Fujieda, N.; Tsutsumi, M.; Tsujimura, S.; Shirai, O.; Kano, K. *Electrochemistry* **2008**, *76*, 600–602.
(38) Hibi, T.; Senda, M. *Biosci. Biotechnol., Biochem.* **2000**, *64*, 1963–1966.
(39) Chemnitius, G. C.; Bilitewski, U. *Sens. Actuators, B* **1996**, *32*, 107–113.
(40) May, K. M. L.; Wang, Y.; Bachas, L. G.; Anderson, K. W. *Anal. Chem.* **2004**, *76*, 4156–4161.
(41) Fraley, A.; Ripp, S.; Sayler, G. S. Bioluminescent bioreporter sensing of foodborne toxins. In Genetically engineered and optical probes for biomedical applications II, Brovko, A.; Bornhop, D.; Raghavachari, R.; Achilefu, S., Eds. Spie-Int Soc Optical Engineering: Bellingham, 2004; Vol. *5329*, pp 132−136.
(42) Loughran, M. G.; Hall, J. M.; Turner, A. P. F.; Davidson, V. L. *Biosens. Bioelectron.* **1995**, *10*, 569–576.
(43) Zeng, K.; Tachikawa, H.; Zhu, Z. Y.; Davidson, V. L. *Anal. Chem.* **2000**, *72*, 2211–2215.
(44) Takagi, K.; Shikata, S. *Anal. Chim. Acta* **2004**, *505*, 189–193.
(45) Ito, T.; Hiroi, T.; Amaya, T.; Kaneko, S.; Araki, M.; Ohsawa, T.; Yamamura, A.; Matsumoto, K. *Talanta* **2009**, *77*, 1185–1190.
(46) Javanbakht, M.; Mohammadi, A.; Ganjali, M. R.; Norouzi, P.; Faridbod, F.; Pirelahi, H. *J. Chin. Chem. Soc.* **2007**, *54*, 1495–1504.
(47) Javanbakht, M.; Ganjali, M. R.; Norouzi, P.; Abdouss, M.; Riahi, S. *Anal. Lett.* **2008**, *41*, 619–639.
(48) Recillas-Mota, J. J.; Bernad-Bernad, M. J.; Gracia-Mora, J. *Pharm. Unserer Zeit* **2009**, *64*, 521–524.
(49) Pietrzyk, A.; Suriyanarayanan, S.; Kutner, W.; Chitta, R.; D'Souza, F. *Anal. Chem.* **2009**, *81*, 2633–2643.
(50) Sekiguchi, Y.; Nishikawa, A.; Makita, H.; Yamamura, A.; Matsumoto, K.; Kiba, N. *Anal. Sci.* **2001**, *17*, 1161–1164.

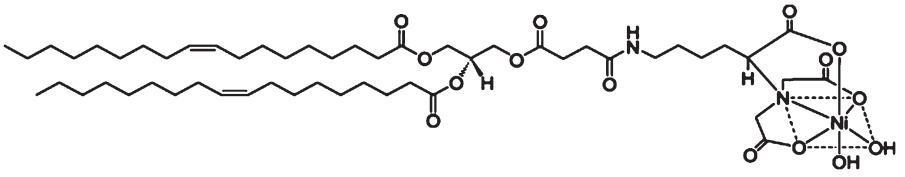

Figure 1. Chemical structure of the chelating lipid (Ni-NTA-DOGS).

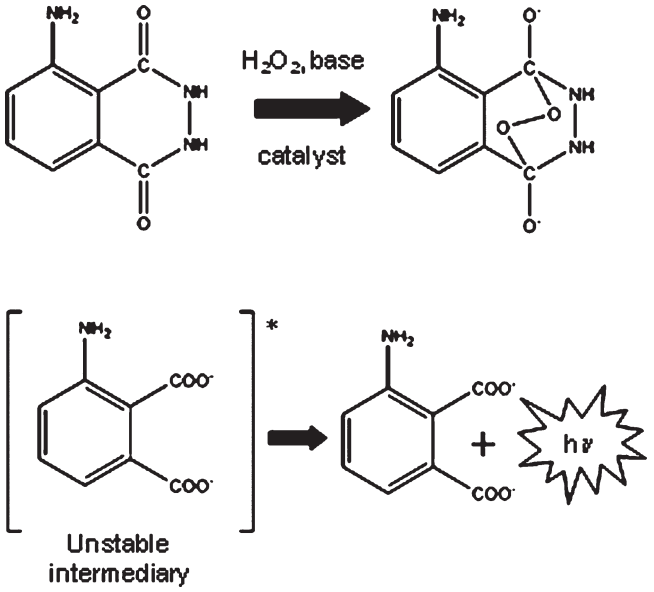

Figure 2. Reaction scheme of the luminol CL reaction.

manganese chloride, sulfuric acid, and hydrogen peroxide (H_2O_2) (30%) AnalaR Normapur were purchased from VWR (France). Copper acetate was obtained from Merck (Germany). 1,2-Dioleyl-*sn*-glycero-3-[*N*-(5-amino-1-carboxypentyliminodiacetic acid) succinyl] (Ni-NTA-DOGS; nickel salt) was provided by Avanti Polar Lipids (Alabaster, AL) (Figure 1). Hellmanex II solution ($Na_3C_6H_9NO_6$ 10−20%, K_3PO_4 20−50%, KOH < 0.5%) was purchased from Hellma (France). Ammonium persulfate, methanol (99.8%), silanization solution I (dimethyldichlorosilane in heptane, v/v: 1/30), nickel chloride, and luminol (5-amino-2, 3-dihydro-1,4-phthalazinedione) were obtained from Sigma-Aldrich (France). A 5.5 mM luminol stock solution was prepared in KOH 10^{-2} M (VWR Prolabo, France).

CL Assays. CL assays were performed with the following final concentrations of the different reactants: luminol 300 μM, H_2O_2 1 mM or 10 mM. Reactions were made in 0.1 M $NaHCO_3$ buffer, pH 10 or 11, the conditions required for a luminol CL reaction catalyzed by metallic cations (reactional mechanism in Figure 2). Light measurements were performed with a luminometer (Luminoskan, LabSystems, USA) and carried out in a 96-well microplate. Fifty microliters of metallic cation solutions (0.1 M) per well were completed to 150 μL with H_2O. CL signals were recorded upon a 150 μL injection of carbonate buffer mixed with luminol and H_2O_2 for 1 min (acquisition time). CL assays on lipids were made under the following conditions: chloroform lipid solution (1.0×10^{-3} M) was diluted 10-fold in methanol; 50 μL of this solution was spread in wells and dried under degreased air flux to obtain coated lipids. To perform nickel/copper ion exchange, 50 μL of a saturated $CuCl_2$ solution (1 mM) was added to the coated lipids per well for 30 min at room temperature. Unbound copper was removed with 5×200 μL water rinses. CL assays were performed by the addition of a 150 μL of a solution of 300 μM luminol and 1 mM H_2O_2 in each well.

CL assays performed on transferred lipid LB films were carried out with a charge-coupled device (CCD) camera (−30 °C) (LAS-1000 plus, Fujifilm, France) under the same reactant concentrations (luminol 300 μM, H_2O_2 1 mM) with a 1 min acquisition time.

Langmuir Film Preparation. Monolayers were prepared on a KSV 2000 LB trough (KSV Instruments, Ltd., Finland) with symmetrical compression system. Surface pressure was controlled by a platinum Wilhelmy plate with an accuracy of ±0.5 mN/m. The lipid solution was prepared in chloroform to a final concentration of 1.0×10^{-3} M. The interfacial films were formed either on ultrapure water 18.2 MΩ·cm pH 5.6 (Milli-Q Plus system, Millipore, France) or on 1 mM copper acetate pH 6.0, respectively, used as the subphase. Experiments were carried out at 20 °C ± 0.5 °C with a water circulating bath (Lauda E100, Lauda France). Forty microliters of lipid solution was spread onto the subphase previously cleaned by suction, using a Hamilton microsyringe. The experimental error on the spread volume gave a standard deviation of ± 0.02 $nm^2 \cdot molecule^{-1}$ for the molecular area. After solvent evaporation (15 min), spread lipids were compressed at a rate of 5 mm/min (i.e., 0.021 $nm^2 \cdot molecule^{-1} \cdot min^{-1}$) up to the desired surface pressure, and the surface pressure isotherm ($\pi-A$) was recorded. After compression and before LB deposition, a ca. 30 min lag time was necessary for the monolayer relaxation.

LB Film Transfer. The transfer of the interfacial film was performed using a vertical LB film deposition procedure on silanized silica substrates. Silica substrates n-type 1.1.1 (Good Fellow, U.K.) were cleaned for 2 h at room temperature within a Hellmanex II bath (2%). After rinses, they were immersed for 30 min under stirring within an ammonium persulfate solution (1%) prepared in sulphuric acid (36 N). Afterward, they were thoroughly rinsed with ultrapure water and carefully dried under a dry air flow. Cleaned silica substrates were dipped for 20 min under stirring in a 2% silanization solution I in chloroform. The silanization only occurred on the substrate silica face because the other one was copper-made. The hydrophobicity degree was estimated by contact angle measurement (Digidrop DGD-DX model, GBX, France). After silanization, the mean contact angle (four replicates) was 73° versus 10° for the untreated substrate (data not shown).

Monolayer depositions were obtained when substrate is pushed at immersion through the compressed monolayer at a transfer rate of 6 mm/min, leading to the transfer of one layer onto the hydrophobic silica with the lipid headgroups pointing outside. The transfer surface pressure was poised at 35 mN/m. After transfer, the substrates were horizontally handled in aqueous medium to avoid any back transfer of the monolayer.

Brewster Angle Microscopy Experiments. Brewster angle microscopy (BAM) allows the characterization of the lipid domain morphology of monolayers at the air/water interface.[51] A Brewster angle microscope (EP3-SW, Nanofilm, Germany) mounted on a Langmuir trough was equipped with a laser (532 nm, 50 mW), a polarizer, an analyzer, and a CCD camera with a x10 magnification lens. The BAM images coded in gray levels were recorded with the CCD scanning camera, using motor control circuitry with a completely hands-off computer-controlled system. The spatial lateral resolution of the microscope was ca. 2 μm and the image size was 483×383 μm. The calibration procedure of the BAM software was used to evaluate the thickness of the layer at the interface. This procedure allows the

(51) Vollhardt, D. *Adv. Colloid Interface Sci.* **1996**, *64*, 143–171.

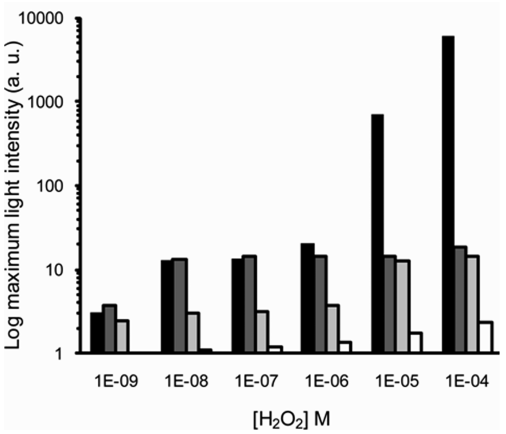

Figure 3. Maximum light intensity as a function of the H_2O_2 concentration (semilog representation) in the presence of different cations: Cu^{2+} (black), Ni^{2+} (dark gray), Zn^{2+} (light gray), and Mn^{2+} (white).

determination of the linear function between the gray level of the images and the reflectance (Rf) of the sample.[52] From the reflectance value, the BAM thickness model allows the evaluation of the layer thickness at the interface with the input of both experimental Brewster angle and optical index of the film. This model is based on the proportional relationship between the reflectance and the square of the interfacial film thickness when the optical index of the film is assumed constant.[53]

AFM. Transferred monolayers were investigated using a commercial AFM (SPM Solver PRO, NT-MDT, Moscow, Russia). After transfer, the substrate was horizontally handled in aqueous medium to avoid any back transfer of the monolayer, rinsed in pure water to remove the subphase, and dried under a degreased air flow until complete evaporation. Topographic images of the transferred monolayer at 35 mN/m were recorded in air either in tapping-mode for image scanning or in contact-mode (scratching) for thickness evaluation with AFM "golden" antimony-doped N-type silicon probe sharpened V-type cantilevers (length 125 μm, NT-MDT, Moscow, Russia) at a scan rate of 1−1.6 Hz.

Results and Discussion

Study of the CL Signal of Luminol with Metallic Cations. Four metallic cations (Cu^{2+}, Ni^{2+}, Zn^{2+}, Mn^{2+}) known to catalyze the CL reaction of luminol were tested in solution.[54] As shown in Figure 3, the catalysis of the luminol CL reaction is efficiently performed in the presence of copper ion.

Immobilized Cation Exchange Investigations. The chelating lipid used in this study was synthesized in the presence of nickel salts (Figure 1). Since luminescence is better catalyzed by copper than nickel, CL measurements were performed on coated lipids in a 96-well microplate in order to check the possibility of exchanging the immobilized cation on the lipid headgroup. Pure Ni-NTA-DOGS or Cu-NTA-DOGS, for which Ni^{2+} had been replaced by Cu^{2+} during a 30 min incubation in a saturated copper solution, were tested. Figure 4 shows that the exchange of the immobilized cation is efficient; the CL signal is increased when Cu^{2+} is immobilized on the lipid chelating headgroup. With a copper ion, the signal-to-noise (S/N) ratio is increased by a factor of 20. This result points out that the copper ion keeps its catalytic efficiency even if it is immobilized on the lipid headgroup.

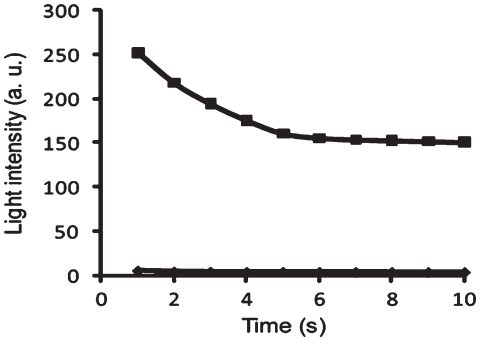

Figure 4. CL signal obtained with coated Ni-NTA-DOGS (triangle) or Cu-NTA-DOGS (formed after exchange of chelated Ni^{2+} cations by Cu^{2+} cations during a 30 min incubation in a saturated $CuCl_2$ solution) (square). The recorded signal is a flash-type signal.

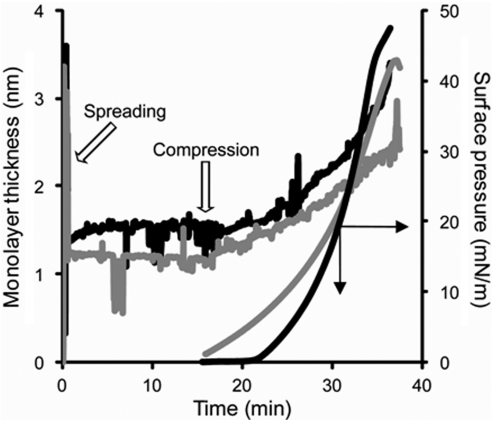

Figure 5. BAM analysis of the change in thickness as a function of time. Zero on the X axis corresponds to the beginning of the spreading procedure. Thickness was calculated from the reflectivity after BAM calibration. Black line: Cu-NTA-DOGS; gray line: Ni-NTA-DOGS.

Ni-NTA-DOGS Interfacial Film Behavior on Pure Water and Copper Acetate Subphases. As mentioned above, the chelating lipid was commercially provided as a nickel salt. So, in order to get the best CL signal of the sensing layer transferred on silica, the immobilized cation (Ni^{2+}) had to be exchanged by copper ion (Cu^{2+}). Several approaches were tested. The best procedure was to spread the Ni-NTA-DOGS on a subphase with 1 mM copper acetate (CuOAc) at pH 6.0, and allow for ion exchange during the initial lag time, which ensures solvent evaporation. Figure 5 shows the BAM analysis of the change in thickness (calculated from the reflectivity after BAM calibration) as a function of time. We can see that the monolayer thickness significantly increases during the first 3 min after spreading and then, remains slightly higher on the CuOAc subphase until the end of the solvent evaporation, compared to the water subphase. This experiment was repeated for 10 and 30 min of evaporation time (data not shown). The same observation was made. In all cases, this first 3 min increase ranges from 1.3 to 1.5 nm on CuOAc subphase, whereas no variation occurs for the monolayer on the pure water subphase, which remains 1.2 nm thick until the compression. Therefore, the exchange between Ni^{2+} and Cu^{2+} cations happens very early during the monolayer formation and modifies the initial packing of the lipid chains. Upon interaction with Cu^{2+} cations, these chains straighten up on the CuOAc subphase.

(52) Winsel, K.; Hönig, D.; Lunkenheimer, K.; Geggel, K.; Witt, C. *Eur. Biophys. J.* **2003**, *32*, 544–552.
(53) de Mul, M. N. G.; Mann, J. A. *Langmuir* **1998**, *14*, 2455–2466.
(54) Badocco, D.; Pastore, P.; Favaro, G.; Macca, C. *Talanta* **2007**, *72*, 249–255.

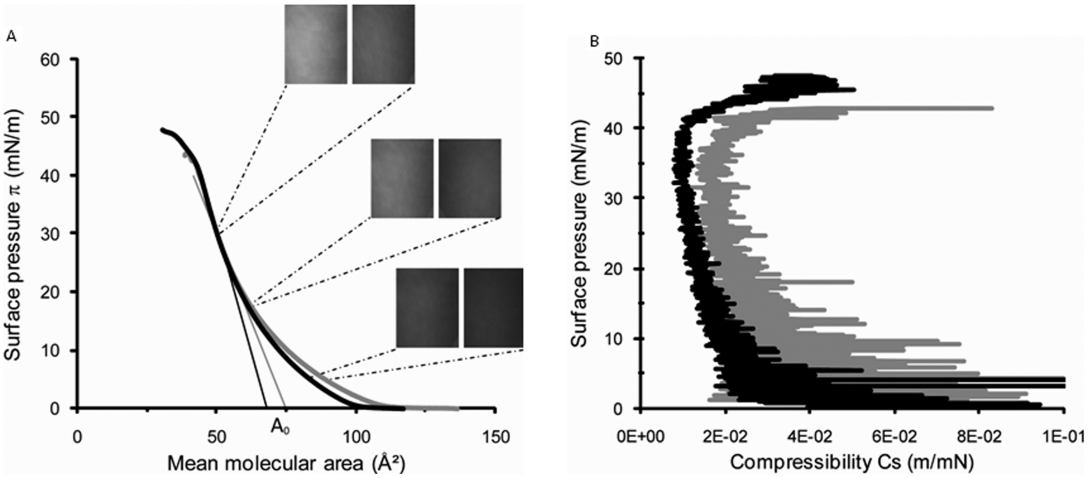

Figure 6. (A) $\pi-A$ isotherms and BAM images of Ni-NTA-DOGS monolayers spread on pure water supplemented (black line) or not (gray line) by 1 mM copper acetate, pH 6.0. BAM images (383 × 483 μm) were taken at 5, 20, and 35 mN/m. For each couple, the picture on the left was taken on copper acetate subphase, and the picture on the right was taken on pure water subphase. (B) Compressibility curves as a function of the surface pressure (mN/m) for monolayers spread on pure water (gray line) or on 1 mM copper acetate pH 6.0 (black line).

Table 1. BAM Data and Monolayer Thickness Estimations at 35 mN/m Using the BAM Model with Experimental Angles of 53.170 and 53.172 for H_2O and CuOAc Subphases, Respectively, and a Refractive Index of 1.47 for Lipid[56]

	gray level	calibration factor	reflectance (Rf)	estimated thickness (nm)
H_2O	67.5	3.91×10^{-8}	2.14×10^{-6}	2.14
CuOAc	115	3.89×10^{-8}	3.90×10^{-6}	2.68

Figure 6A shows the interfacial behavior of Ni-NTA-DOGS monolayers formed on different subphases. On pure water (gray curve), surface pressure regularly increases up to a collapse pressure at ~43 mN/m (i.e., 35 Å^2/lipid molecule), with a takeoff point of 118 ± 2 Å^2/lipid molecule and a limiting mean molecular area (A_0) of 74 Å^2/ lipid molecule. All over the compression, the lipid monolayer remains in fluid phase. The 2D compressibility defined as $Cs = -1/A(dA/d\pi)_T$ has been plotted as a function of the surface pressure. The compressibility curve shows a regular decrease all along the monolayer compression until the collapse pressure. At 35 mN·m^{-1} (transfer surface pressure), the Cs value equal to 0.018 m.mN^{-1} corresponds, according to Davies and Rideal,[55] to an undefined phase between the liquid-expanded and the liquid-condensed ones.

On 1 mM copper acetate subphase (black curve), the global shape of the isotherm diagram remains unchanged, but some discrepancies can be noticed: (i) the takeoff point is obtained at a lower molecular area (100 ± 2 instead of 118 ± 2 Å^2/lipid molecule), and (ii) the isotherm curve is shifted toward smaller areas at the beginning of the compression, due to the initial packing chain modified by the interaction with Cu^{2+}. The collapse pressure is nearly the same as on pure water (~45 instead of 43 mN/m, Figure 6A), but the compressibility is slightly lower (Figure 6B). On CuOAc subphase, the Cs values are closer to the condensed phase[55] at the end of the compression.

BAM Monolayer Characterization before Transfer. Homogeneity of lipid monolayers has been characterized before transfer onto silica substrate both on pure water and acetate copper subphases. BAM images reveal that the monolayers are in an expanded phase all over the compression (no condensed apparition domains visible) (Figure 6A). The main difference between the two sets of measurements takes place in the Reflectance values (Rf), increasing from Rf = 2.14×10^{-6} to Rf = 3.90×10^{-6} at 35 mN/m (transfer pressure), respectively, for the monolayer spread on pure water and for the monolayer spread on supplemented copper subphase (Figure 6A and Table 1).

Taking a refractive index of 1.47,[56] the monolayer thickness estimations, through the BAM calibration procedure and thickness model, give ca. 2.1 nm and ca. 2.7 nm for monolayers on water and copper acetate subphases, respectively. This difference has been ascribed to the effects of both copper and acetate ions in the subphase, which have a compacting effect by decreasing charge repulsion between the lipid headgroups. This statement corroborated a smaller takeoff area per molecule observed on the $\pi-A$ isotherm diagram recorded on supplemented copper subphase, which has been related to the initial packing change modification upon Cu^{2+} interactions.

Transfer onto Silica Substrate and AFM Characterization. Monolayer transfer proceeded from the dipping of silanized silica substrate through the monolayer at a 35 mN/m surface pressure. Monitored transfer plots show a reproducible [transfer ratio = 0.5 ± 0.1 (only one face of the substrate is silanized since the other side is copper-made)] and a relatively homogeneous transfer along the substrate, whatever the subphase nature (data not shown). These macroscopic observations have been confirmed by AFM characterization (Figure 7), which reveals a good homogeneity of the supported monolayer, without defects in the lipid organization whatever the immobilized cation, Ni^{2+} (data not shown) or Cu^{2+}.

A thickness of 2.3 ± 0.3 nm has been estimated on scratched film (data not shown). This value corroborates the interfacial monolayer one evaluated by BAM calculation model before transfer.

CL Assays on Transferred Monolayers. Transferred monolayers were placed in a cell in which the reactant solution was added. CL signal was monitored for a 1 min acquisition time with a CCD camera. Figure 8 shows the results obtained for Ni-NTA-DOGS monolayers transferred onto a silica substrate from either a pure water (on the left) or a 1 mM copper acetate subphase (on the right).

During the monolayer formation on the copper acetate subphase, Ni^{2+} cations, initially immobilized on the lipid polar headgroup, were exchanged with Cu^{2+} cations present in the

(55) Davies, J. T.; Rideal, E. K. Properties of monolayers. In *Interfacial Phenomena*, 2nd ed.; Academic Press: New York and London, 1963; p 265.

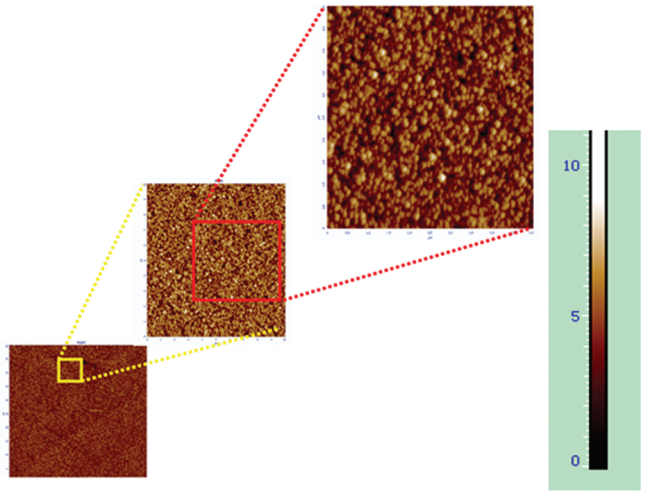

Figure 7. AFM tapping mode pictures (from the left to the right: 50 × 50; 10 × 10; 5 × 5 μm^2) of a transferred Cu-NTA-DOGS monolayer formed on 1 mM copper acetate subphase.

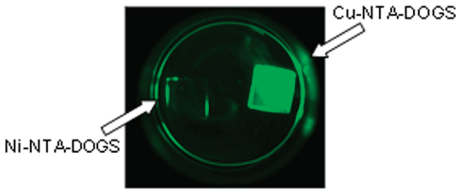

Figure 8. CL signal of transferred silica substrate observed with a CCD camera (time acquisition: 1 min). On the left side, substrate with transferred Ni-NTA-DOGS on water subphase; on the right side, Cu-NTA-DOGS transferred onto a 1 mM copper acetate subphase (chelated Ni^{2+} exchanged with subphase Cu^{2+}). CL conditions: [luminol] = 300 μM; [H_2O_2] = 1 mM; carbonate buffer 0.1 M pH 11.

subphase at a saturated concentration. After deposition onto a silica substrate, the transferred monolayer was rinsed with ultrapure water (5 × 20 mL) to remove the unbound copper ions. As shown in Figure 8, the CL signal, homogeneous along the substrate, is strongly enhanced after replacement of Ni^{2+} by Cu^{2+}. As a control, a Ni-NTA-DOGS monolayer compressed on a 1 mM $NiCl_2$ subphase was transferred onto a silica plate. The CL signal obtained was similar to that obtained for the Ni-NTA-DOGS monolayer formed on pure water. When no lipids are present on the substrate, no CL signal is recorded (data not shown). Thus, these results clearly evidence that the luminol CL reaction is efficiently catalyzed by Cu^{2+} cations immobilized on the chelating lipid. Even though we have shown that the cation exchange starts early during the monolayer formation, we performed CL assays on different transferred monolayers compressed after several evaporation times (i.e., 10, 15, and 30 min) in order to be sure that the cation exchange was optimal. Figure 9 evidences that a 15 min-evaporation time is enough to reach 97% of the maximum CL signal.

CL Signal Variation upon Histamine Interaction. In order to demonstrate the CL signal variation upon molecular interactions mediated by the imidazole ring on the supported monolayer, histamine was used as a model taking into account its importance as a biomarker for food quality control. In the experiments, the CL reaction buffer was changed by decreasing the pH from 11 to

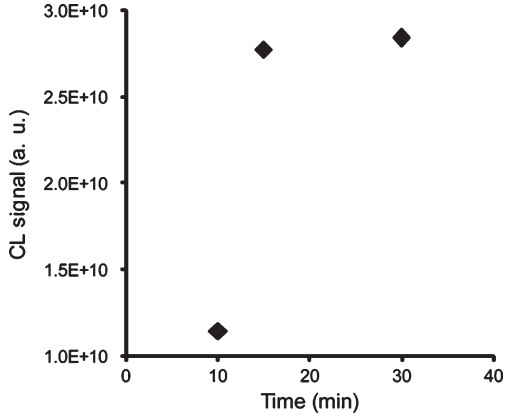

Figure 9. CL signal measurement as a function of the evaporation time.

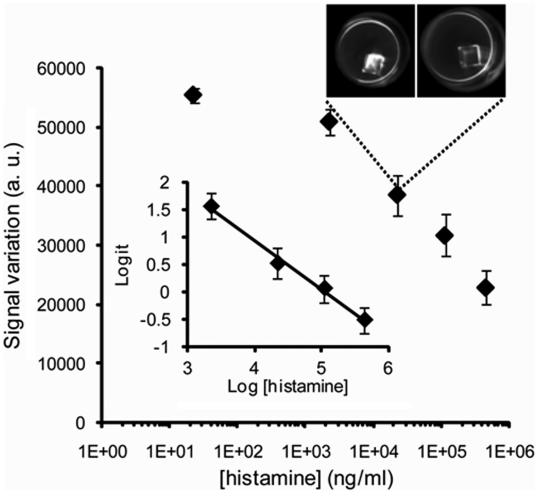

Figure 10. CL signal variation as a function of the histamine concentration (semilog representation). Results are obtained by subtracting the reference CL signal from the CL signal recorded after histamine incubation (30 min, room temperature, under stirring). For the highest histamine concentration, pictures of the CL signal are taken before (left side) and after (right side) histamine incubation. The difference between the two signals is directly reported as Δ light intensity (a.u.). CL conditions: [luminol] = 300 μM; [H_2O_2] = 10 mM; carbonate buffer 0.1 M pH 10. Experimental error bar was calculated with a set of two repeated measurements. Inset: logit as a function of histamine concentration; R^2 = 0.992.

10 to improve monolayer stability, and by increasing the H_2O_2 concentration from 1 mM to 10 mM to compensate for the signal loss due to the pH reduction. For all experiments, the reference CL signal was recorded on the supported monolayer. The incubation with histamine using freshly prepared solutions in ultrapure water at various concentrations was then achieved (30 min, at room temperature, under stirring). After incubation, the substrate was meticulously rinsed with ultrapure water, and a second CL signal was recorded. The calibration curve (CL signal variation obtained by subtracting the reference signal to the assay value) and its logit linearization are presented in Figure 10.

The logit representation is calculated as follows: logit = $\ln(I/[I_0 - I])$, where I_0 is the maximum signal obtained in the absence of histamine (I_0 = 61 509 a.u.) and I is the signal obtained in its presence. The results show that the presence of histamine could be detected at a concentration of 2 μg/mL [sensitivity = 0.41 au/(ng·ml^{-1})] with a range from 2 to 4.44 × 10^3 μg/mL,

(56) Castano, S.; Delord, B.; Février, A.; Lehn, J.-M.; Lehn, P.; Desbat, B. *Langmuir* **2008**, *24*, 9598–9606.

Table 2. Different Histamine Sensor Characteristics

sensor type	reference	LOD	dynamic range
whole-cell	41	100 μM	
whole-cell	40	10−100 μM	
amperometric	37		2−30 μM
amperometric	38	0.1 μM	
amperometric	39		0.17−20 μM
amperometric	42	4−8 μM	0−200 μM
amperometric	43		25 μM to 4 mM
FIA	44	5 μM	over 0.6 mM
FIA	45		1 μM to 1 mM
ISE	47	1 μM	2.5 μM to 100 mM
ISE	46	3 μM	5 μM to 100 mM
MIP	49	5 nM	10−100 mM
CL	50	0.08 μM	0.1−50 μM

i.e., 18 μM to 40 mM. For the limit of detection (LOD; 2 μg/mL), the mean I value of two replicates was 50 900 a.u. (with a 4400 standard deviation and a relative standard deviation equal to 8.6%).

Compared with other detection systems (Table 2), the LOD and the dynamic range of the developed system in this work are not so different from enzyme-based amperometric biosensors.[37,39,42] The detection limits are usually around 0.5−10 μM,[57] even in FIA.[44] It is noteworthy that Hibi and Senda reported an LOD of 0.1 μM for amperometric detection of histamine using a histamine oxidase/peroxidase based sensor.[38]

The dynamic range is narrow in most histamine sensor implementations reported so far and does not extend beyond a few tens of micromolars[37,39] depending on the enzyme immobilization method, except for the amperometric detection of histamine with a methylamine dehydrogenase polypyrrole-based sensor for which Zeng et al. reported a dynamic range of 25 μM to 4 mM.[43] It must be stressed that the results obtained with whole-cell based biosensors present a same magnitude order for the detection limit, but the dynamic range increases until ca. 100 μM.[40,41] Except for recognition by MIPs[49] for which the lowest LOD was reported (5 nM), the ion selective electrodes (ISEs)[46,47] give a dynamic range (5 μM to 100 mM), similar to the one reported here.

To our knowledge, only one CL sensor has been reported. This sensor using immobilized histamine oxidase and peroxidase presents a low detection limit (0.08 μM) and a dynamic range of 0.1 μM to 50 μM.[50] Even if such a sensitivity is not reached for the moment, chelating CL LB films are based on a detection system that is not dependent on enzyme activity (sensitive to the inactivation), that avoids any enzyme immobilization, and that allows label-free detection.

Conclusions

The main accomplishment of this work was to design a new CL sensing layer tailored for the label-free detection of molecules by direct interaction on the chelating lipid headgroup of a thick organized LB film. The main advantage of such a sensing layer is that the supported monolayer simultaneously plays an active role in immobilization and detection processes. As a proof of concept, we used histamine as a model. As demonstrated, this layer can (i) retain molecules including an imidazole ring by chelation mediated by a metallic cation on a Cu−NTA functional lipid headgroup and (ii) allow the quantification of the immobilized molecule without label, thanks to a sensitive variation of the emitted CL signal in a concentration-dependent manner.

As it is designed, this sensing layer is versatile. Different kinds of His-tagged receptors can be immobilized and will further serve for investigation of protein−ligand interactions. In this case, a new signal variation will be expected after bioreceptor/ligand interactions. The development of the immobilization matrix is based on self-assembled properties of lipid molecules. Hence, as it is organized at the molecular scale, small highly ordered areas can be generated, allowing effective miniaturization.

Finally, this sensing layer will be exploited for the achievement of a pluripotent sensor able to catalyze by itself the luminol CL reaction. This new sensing layer provides a good compromise between cost and sensitivity to finally reach a highly efficient label-free detection method.

Acknowledgment. This work is partly supported by CNRS and by the French Research Ministry (MRT, Ministère de la Recherche et Technologie) for the Ph.D. fellowship of A.A.-M.S.

(57) Kivirand, K.; Rinken, T. *Anal. Lett*. **2009**, *42*, 1725–1733.